SAND2011-2776C

Optimal Power Flow with Application to Renewable Energy Grid Integration

Matthew Heath, Gordon Parker, David G. Wilson, and Rush D. Robinett III

***Abstract*— Developing requirements for renewable power sources that are able to meet specified load needs is the motivation for this work. The approach used here is to formulate energy storage as an optimal control problem. Alternative objective functions are applied to a tutorial LC circuit yielding insight into the relationship between the supply characteristics and the rate of storage. Given a specified storage target and time, several objective functions are considered. These are used to form a spectrum of voltage source time histories that minimize the objective functions while achieving the storage target. Although the system being considered is linear, the complexity of the solutions arises due to the nonlinearity of the objective functions employed. The resulting source characteristics provide insight into desirable renewable source characteristics. More importantly, this work describes a methodology for addressing more complex renewable integration designs using an optimal control approach.**

I. INTRODUCTION

A microgrid is a modular version of a traditional power grid containing the key elements of generation, transmission, distribution, controllable loads, storage, and separability from other power grids. Microgrids are envisioned that are scalable, and when connected together will have the same functionality as a large, regional power grid. Introduction of renewable sources poses a particular challenge for microgrids due to their variability (e.g. wind and photovoltaic sources) and potential for causing grid voltage instability when they become a large portion (roughly greater that 20%) of the overall electrical supply. Increasing the amount of storage is one expensive solution approach to facilitate high-penetration renewables in a microgrid while maintaining stability. Microgrid design and analysis methods that minimize storage, maximize renewables and maintain stability are therefore of great interest.

Network power flow has been considered in many previous studies with a nice summary provided by the recent paper by Pandya and Joshi [2]. This work differs from network analysis by focusing on the transient behavior associated with charging. Similar pulse solution were examined in the paper by Beccuti et al. for optimal control of a boost converter [1].

M. Heath is a M.S. student in the Department of Mechanical Engineering - Engineering Mechanics, Michigan Technological University, Houghton, MI 49931, USA mjheath@mtu.edu

G. Parker is with the Department of Mechanical Engineering - Engineering Mechanics, Michigan Technological University, Houghton, MI 49931, USA ggparker@mtu.edu

D. Wilson is with Water Power Technologies Department , Sandia National Laboratories, Albuquerque, NM 87185, USA dwilso@sandia.gov

R. Robinett is with Operational Energy Security Group, Sandia National Laboratories, Albuquerque, NM 87185, USA rdrobin@sandia.gov

Optimization will be an important part of microgrid design when considering high-penetration renewables. The focus of this work is the optimal charging of a capacitor in a very simple circuit consisting of a voltage source, an inductor and a capacitor, described by the differential equation of Eq. 1. The source input, $v(t)$, is assumed to be a series of n time-delayed steps as shown in Eq. 2 where $h(t)$ is the unit step function. The final time, t_f, and final charge level, q_f, are specified.

$$L\ddot{q}(t) + \frac{1}{C}q(t) = v(t) \tag{1}$$

$$v(t) = \sum_{i=1}^{n} A_i \cdot h(t - T_i) \tag{2}$$

The remainder of the paper will use well-known results for generating the constraint equations on the discontinuous input parameters, A_i and T_i, such that q_f is achieved at $t = t_f$ with $\dot{q}(t_f) = 0$. By selecting n larger than the minimum value required to achieve a solution, the opportunity to select the parameters of $v(t)$ to minimize particular cost functions is created.

II. OPTIMIZATION PROBLEM DESCRIPTION

By defining nondimensional time as $\tau \equiv \frac{\omega t}{2\pi}$ with $\omega = \sqrt{1/(LC)}$ the nondimensional form of Eq. 1, a simple harmonic oscillator, can be written as shown in Eq. 3.

$$q''(\tau) + (2\pi)^2 q(\tau) = (2\pi)^2 \bar{v}(\tau) \tag{3}$$

where $q''(\tau)$ is the second derivative of q with respect to τ and $\bar{v} \equiv Cv$. Note that the units of q and $\bar{v}$ are both Coulombs in this nondimensional time form. Given values for τ_f and q_f and assuming the form of $\bar{v}$ given by Eq. 4 the optimization problem is to find the A_i and T_i such that $q(\tau_f) = q_f = 1$, $\dot{q}(\tau_f) = 0$ and the cost function is minimized. We will also constrain $\tau_f < 1$ which means that the final charge time will be less than one period of oscillation.

$$\bar{v}(\tau) = \sum_{i=1}^{n} A_i \cdot h(\tau - T_i) \tag{4}$$

Several cost functions will be examined where we note that the supply power is $P_s(\tau) = \bar{v}(\tau)q'(\tau)$ and its energy provided to the circuit is $E_s(\tau) = \int_0^\tau P_s(\chi)d\chi$. Next we'll look at four different cost functions, and justify narrowing the field to three based on the structure of the optimization problem.

Consider first the optimal energy cost function given in Eq. 5. Since the final state condition, $q'(\tau_f) = 0$ is imposed, the energy in the inductor, $E_L(\tau) = \frac{1}{2}Lq'(\tau)^2$ at $\tau = \tau_f$ will be zero. Since there are no losses in the circuit, all the energy extracted from the supply has been put into the capacitor to achieve the end state of $q(\tau_f) = q_f = 1$. So, J_{energy} is only a function of τ_f and is independent of the free parameter T_2. Minimization of J_{energy} will not be considered further.

$$J_{energy} = \int_0^{\tau_f} \bar{v} q' d\tau \tag{5}$$

The remaining three cost functions are shown in Eq. 6. The first objective function, $J_{\bar{v}}$, is a measure of the normalized total supply effort whereas the second two functions measure normalized power supplied. The units for the three objective functions, from top to bottom, are C^2, C^4, and C^2 where C in this context denotes Coulombs.

$$\begin{aligned} J_{\bar{v}} &= \int_0^{\tau_f} \bar{v}^2 d\tau \\ J_{P^2} &= \int_0^{\tau_f} P_s^2 d\tau \\ J_{P_{max}} &= \max_{\tau}(P_s) \end{aligned} \tag{6}$$

Now that the optimization problem has been defined, a brief review of input shaping is given in terms of its relationship to helping to find the $\bar{v}$ step sequence that minimizes the objective functions of Eq. 6.

Input shaping is a method to generate input commands to move oscillatory systems while guaranteeing zero residual oscillation [3]. By solving for the system response to a set of parameterized impulses, several constraint equations can be developed that will ensure zero residual oscillation. The same approach is used here. Instead of simply stating the constraints, a brief overview of their development is provided.

The constraints on A_i and T_i of Eq. 4 are readily found by forming the solution to Eq. 3 and then requiring that $q(\tau) = 1 \quad \forall \tau \geq \tau_f$. This solution is given in Eq. 7 after factoring with respect to $\sin 2\pi\tau$ and $\cos 2\pi\tau$.

$$\begin{aligned} \left(\sum_{i=1}^{n} A_i - 1\right) + \left(\sum_{i=1}^{n} A_i \sin(2\pi T_i)\right) \cos(2\pi\tau) + \\ + \left(\sum_{i=1}^{n} A_i \cos(2\pi T_i)\right) \sin(2\pi\tau) = 0 \end{aligned} \tag{7}$$

Eq. 7 gives the three necessary conditions for achieving the optimization problem solution listed in Eq. 8. A fourth condition is simply that $T_n = \tau_f$.

$$\begin{aligned} T_n - \tau_f = 0, \quad \sum_{i=1}^{n} A_i - 1 = 0 \\ \sum_{i=1}^{n} A_i \sin(2\pi T_i) = 0, \quad \sum_{i=1}^{n} A_i \cos(2\pi T_i) = 0 \end{aligned} \tag{8}$$

If the first step starts at $T_1 = 0$ and the first two constraints of Eq. 8 are used to resolve out T_n and A_1, then we have $2n - 3$ parameters to select and two remaining constraints from Eq. 8. The case of $n = 2$ leaves only one parameter and two constraints. This is solvable for a particular value of $\tau_f = 0.5$. Unwinding the nondimensionalization yields the very familiar result of ending the charging at the half-period time.

The problem considered here is for the general τ_f case where a minimum of $n = 3$ steps are needed. This gives three parameters to solve the remaining two constraints of Eq. 8. This remaining degree of freedom can be used to achieve achieve either of the minimization objectives.

Now that we are focusing on the three step solution the constraints can be written explicitly as given in Eq. 9.

$$\begin{aligned} A_1 + A_2 \cos(2\pi T_2) + A_3 \cos(2\pi\tau_f) = 0 \\ A_2 \sin(2\pi T_2) + A_3 \cos(2\pi\tau_f) = 0 \\ 1 - A_1 - A_2 - A_3 = 0 \end{aligned} \tag{9}$$

The three expressions in Eq. 9 can be combined into the two constraints of Eq. 10.

$$\begin{aligned} A_2 [-1 + \cos(2\pi T_2)] + A_3 [-1 + \cos(2\pi\tau_f)] = -1 \\ A_2 \sin(2\pi T_2) + A_3 \cos(2\pi\tau_f) = 0 \end{aligned} \tag{10}$$

The optimization problem can now be parameterized in the single quantity T_2 which is the start time of the second pulse. The optimal value of T_2 is easily found by sweeping through values of T_2 within $[0, \tau_f]$ and selecting the one that gives the minimum value of the three cost functions of Eq. 6. For each value of T_2, the corresponding values of A_2 and A_3 are readily solved from Eq. 10. The value of A_1 can then be obtained from the last expression in Eq. 9.

Before moving on to the results section it should be noted that the $n > 3$ case was also investigated using a numerical optimization code. For all the cases considered the parameters converged to a solution that eliminated all but three steps. Though this result is only anecdotal it provided some justification for considering the three step scenario.

III. RESULTS

A MATLAB simulation of the system was created to find the optimal T_2 values. The solver was a fixed-time, fourth order Runge-Kutta with a time step of 0.0001 seconds. The excessively small time step was merely to allow four digit discrimination of T_2 values. Seventeen final time cases were examined over $[0.1, 0.9]$ in increments of 0.05. For each τ_f the T_2 parameter was swept between $[0.01, \tau_f - 0.01]$ using 60 increments while computing the $J_{\bar{v}}$, J_{P^2} and $J_{P_{max}}$ objective functions for each case. Finally, the T_2 value corresponding to the minimum value for each objective function was extracted. These results are shown in Table I. A sample time history of the input and output is shown in Figure 1.

The minimum values of J_{P^2} and $J_{P_{max}}$ are not shown in Table I since they have a very expected trend of decreasing

as τ_f increases. The values of $J_{\bar{v}}$ are shown in Figure 2 where a distinct minimum is evident in the $\tau_f < 0.5$ region. It's clear that if small τ_f is required, an optimal value of about 0.45 is desirable. It should be noted that the sensitivity of $J_{\bar{v}}$ is high in this region. Uncertainty in system L and C parameters could result in undesirably large $J_{\bar{v}}$. Thus a more conservative value of $\tau_f = 0.6$ would be a better choice.

TABLE I

OPTIMAL SECOND PULSE TIME, T_2, FOR ALL $0.1 \leq \tau_f \leq 0.9$

	T_2		
τ_f	Effort	Power	Max Power
0.10	0.050	0.050	0.053
0.15	0.075	0.075	0.084
0.20	0.103	0.100	0.121
0.25	0.129	0.121	0.167
0.30	0.164	0.127	0.220
0.35	0.214	0.093	0.285
0.40	0.276	0.061	0.358
0.45	0.368	0.024	0.433
0.50	0.000	0.000	0.000
0.55	0.072	0.363	0.363
0.60	0.097	0.387	0.397
0.65	0.126	0.399	0.409
0.70	0.146	0.418	0.418
0.75	0.168	0.424	0.424
0.80	0.218	0.439	0.439
0.85	0.273	0.453	0.453
0.90	0.347	0.465	0.465

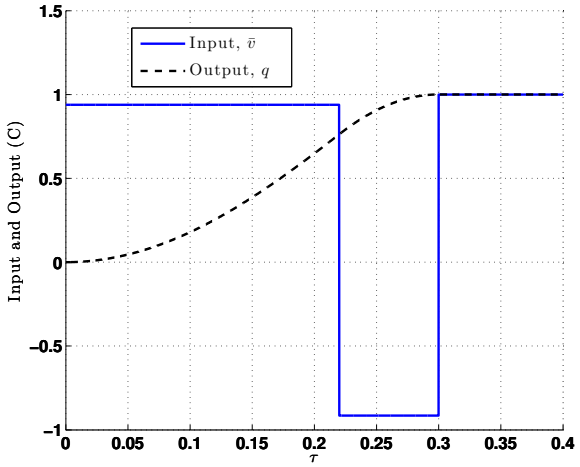

Fig. 1. Sample input, $\bar{v}$, and output, q, for the $\tau_f = 0.3$ case. The value of T_2 is 0.220, and is the optimal $J_{P_{max}}$ solution.

Figure 3 shows the shape of all three objective functions as T_2 is swept from low to high values. The T_2 optimal values are shown with the square, circle, and dot markers for minimum effort, power, and maximum power. For this case of $\tau = 0.3$ the objective functions have well defined extremums. It should be noted that for some values of τ_f the objective functions have local extremums, and for others the extremum is at a boundary point.

Figure 4 compares the optimal T_2 values as a function of τ_f for all three objective functions. The value of T_2 has been further normalized by dividing by τ_f. This provides more

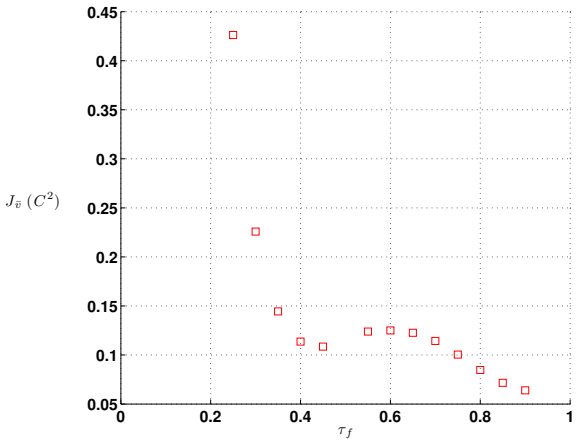

Fig. 2. The optimal $J_{\bar{v}}$ values for $0.25 \leq \tau_f \leq 0.9$ where a local minimum occurs at $\tau_f \approx 0.45$.

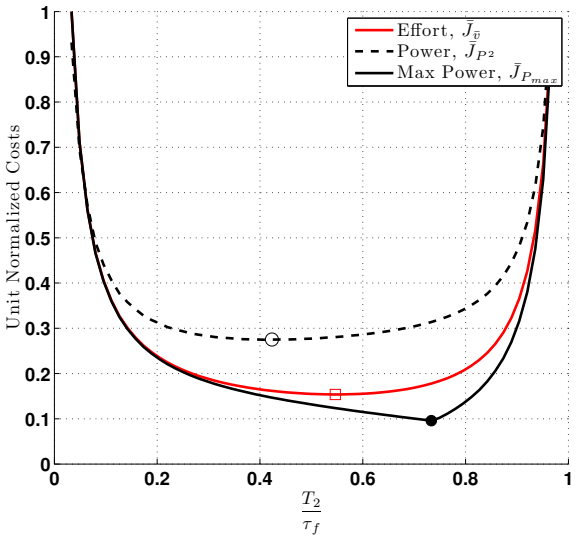

Fig. 3. Comparison of all three objective functions evaluated for all T_2 sweep values for the example case of $\tau_f = 0.3$. The square, circle, and dot show the location of the maximum values. The costs have been normalized, indicated by the $\bar{J}_i$ notation, allowing the cost function shapes to all be seen on one figure.

insight into where T_2 occurs relative to the entire charging time. The T_2 values corresponding to optimal power are shown as dots and open circles whereas the effort optimal T_2 values are given squares. For fast charging, $\tau_f < 0.2$, all three solutions indicate an optimal T_2 that is between $50\% - 60\%$ of τ_f. For $0.2 \leq \tau_f \leq 0.5$ the optimal effort and maximum power values of T_2 increase and approach τ_f. In contrast, the power optimal solution indicates small values of T_2 that approach zero as $\tau_f \to 0.5$. The $\tau_f = 0.5$ case is the singular solution where only two steps can be used. It is also a transition point for the structure of the optimal values of T_2 for all three objective functions. For $\tau_f > 0.5$ the two power related objective functions yield the same solution whereas the effort optimal T_2 moves from roughly 10% of τ_f up to 40% of τ_f by $\tau_f = 0.9$.

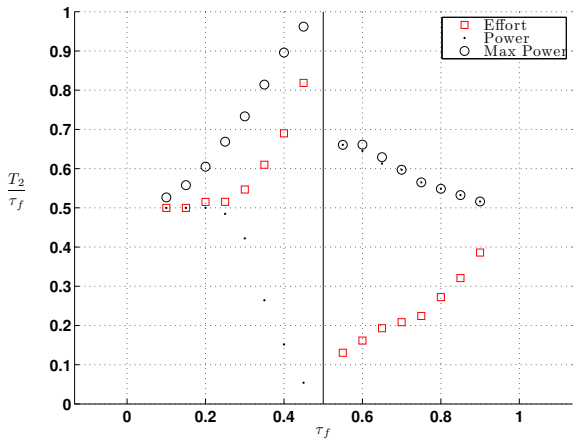

Fig. 4. Normalized T_2 as a function of the final charging time τ_f for all three objective functions.

IV. CONCLUSIONS

Optimal capacitor charging was investigated where the input was postulated as being discontinuous, leaving only one free parameter. This allowed the calcuation of the globally optimal solution for the three cost functions of Eq. 6 to be found. The solutions are all quite different, but from a practical perspective, the most useful is likely the $J_{P_{max}}$ case. This allows the capacitor to charge within the specified time while keeping the maximum power requirement for the supply as low as possible. When τ_f approaches the half-period value, T_2 approaches zero. Thus the three step input degrades to two. It is interesting that the maximum power solution and the integrated power squared solutions are the same for τ_f greater than the half-period value.

Although this is very simple example, the approach can be readily applied to more complex storage charging scenarios. It's very likely that an $n > 3$ number of steps would be needed to accommodate multiple mode systems. It should be noted that the constraint equations of Eq. 8 can be extended to systems with m natural frequencies as given by Eq. 11 resulting in $2(1+m)$ equations and $2n-1$ unknowns if the first pulse starts at $t = 0$. The quantities in Eq. 11 are not nondimensionalized since there are multiple ω_i in the equations.

$$\begin{aligned} &T_n - t_f = 0 \\ &\sum_{i=1}^{n} A_i - q_f = 0 \\ &\sum_{i=1}^{n} A_i \sin(\omega_j T_i) = 0,\ j = 1 \ldots m \\ &\sum_{i=1}^{n} A_i \cos(\omega_j T_i) = 0,\ j = 1 \ldots m \end{aligned} \tag{11}$$

REFERENCES

[1] A. G. Beccuti, G. Papafotiou, and M. M., "Optimal control of the boost dc-dc converter," in *Proceedings of the 44th IEEE Conference on Decision and Control*, 2005, pp. 4457–4462.

[2] K. S. Pandya and S. K. Joshi, "A survey of optimal power flow methods," *Journal of Theoretical and Applied Information Technology*, vol. 4, no. 5, pp. 450–458, 2008.

[3] N. C. Singer and W. P. Seering, "Preshaping command inputs to reduce system vibration," *Journal of Dynamic Systems, Measurement, and Control*, vol. 112, pp. 76–82, March 1988.